Axonal transport of mitochondria requires milton to recruit kinesin heavy chain and is light chain independent

Elizabeth E. Glater,[1,2,3] Laura J. Megeath,[1,2,3] R. Steven Stowers,[4] and Thomas L. Schwarz[1,2,3]

[1]Neurobiology Program, [2]Department of Neurology, and [3]Department of Neurobiology, Children's Hospital, Harvard Medical School, Boston, MA 02115
[4]Department of Molecular and Cellular Biology, University of California, Berkeley, Berkeley, CA 94720

Mitochondria are distributed within cells to match local energy demands. We report that the microtubule-dependent transport of mitochondria depends on the ability of milton to act as an adaptor protein that can recruit the heavy chain of conventional kinesin-1 (kinesin heavy chain [KHC]) to mitochondria. Biochemical and genetic evidence demonstrate that kinesin recruitment and mitochondrial transport are independent of kinesin light chain (KLC); KLC antagonizes milton's association with KHC and is absent from milton–KHC complexes, and mitochondria are present in *klc* $^{-/-}$ photoreceptor axons. The recruitment of KHC to mitochondria is, in part, determined by the NH_2 terminus–splicing variant of milton. A direct interaction occurs between milton and miro, which is a mitochondrial Rho-like GTPase, and this interaction can influence the recruitment of milton to mitochondria. Thus, milton and miro are likely to form an essential protein complex that links KHC to mitochondria for light chain–independent, anterograde transport of mitochondria.

Introduction

Mitochondrial localization and transport ensure the proper inheritance of mitochondria upon cell division (Pereira et al., 1997; Yaffe, 1999) and position mitochondria where energy demands or oxygen supplies are greatest (Hollenbeck and Saxton, 2005). It is likely that the concentration of local cytoplasmic Ca^{2+} also depends on mitochondrial Ca^{2+} uptake (Werth and Thayer, 1994; Zucker, 1999). Consequently, mitochondria accumulate in subcellular regions with high metabolic requirements and high Ca^{2+} influx (Morris and Hollenbeck, 1993) and redistribute in response to changes in the local energy state (Wong-Riley and Welt, 1980; Hollenbeck, 1996). The transport of mitochondria is particularly vital in neurons because of their extended processes, and the disruption of mitochondrial transport is correlated with neurodegenerative disease (Hollenbeck and Saxton, 2005).

The mechanisms of mitochondrial transport differ between species and can require actin, microtubule attachment, or kinesins (Yaffe et al., 2003; Boldogh et al., 2005; Hollenbeck and Saxton, 2005). In metazoans, mitochondrial motility involves both actin- and microtubule-dependent mechanisms (Morris and Hollenbeck, 1995; Hollenbeck, 1996; Ligon and Steward, 2000b; Hollenbeck and Saxton, 2005). In particular, plus end–directed movement involves conventional kinesin (kinesin-1) motors (Hurd and Saxton, 1996; Tanaka et al., 1998; Pilling et al., 2006), although kinesin-3 motors are also implicated (Nangaku et al., 1994; Wozniak et al., 2005). Little is known about how mitochondrial kinesin is regulated or coupled to the organelle (Rintoul et al., 2003; Chada and Hollenbeck, 2004; Miller and Sheetz, 2004; Cai et al., 2005; Hollenbeck and Saxton, 2005; Malaiyandi et al., 2005; Minin et al., 2006).

We recently identified a novel protein called milton, which is required for mitochondrial transport within *Drosophila melanogaster* photoreceptors (Stowers et al., 2002). Mitochondria were absent from *milton* (*milt*) photoreceptor axons, but were normally distributed and appeared to be functional in their cell bodies. Although devoid of mitochondria, their axons and synapses were otherwise surprisingly normal in their general architecture, possessing microtubules, synaptic vesicles, and active zone specializations. Thus, the transport defect was selective for mitochondria (Stowers et al., 2002; Gorska-Andrzejak et al., 2003). The mechanism of milton's action was unknown, but milton was associated with mitochondria and coimmunoprecipitated with kinesin heavy chain (KHC)

E.E. Glater and L.J. Megeath are co-first authors.

Correspondence to Thomas L. Schwarz: Thomas.Schwarz@childrens.harvard.edu

Abbreviations used in this paper: GRIF, γ-aminobutyric acid A receptor–interacting factor; HEK, human embryonic kidney; KHC, kinesin heavy chain; KLC, kinesin light chain; OGT, *O*-GlcNAc transferase; OIP, *O*-linked *N*-acetylglucosamine–interacting protein.

The online version of this article contains supplemental material.

The Journal of Cell Biology, Vol. 173, No. 4, May 22, 2006 545–557
http://www.jcb.org/cgi/doi/10.1083/jcb.200601067

Supplemental Material can be found at:
http://www.jcb.org/cgi/content/full/jcb.200601067/DC1

in extracts of fly heads (Stowers et al., 2002). The mammalian homologues milton 1 and 2, which are also called *O*-linked *N*-acetylglucosamine–interacting protein 106 (OIP106) and γ-aminobutyric acid A receptor–interacting factor-1 (GRIF-1), also colocalize with mitochondria and coimmunoprecipitate with KIF5B, which is a mammalian homologue of *D. melanogaster* KHC (Beck et al., 2002; Iyer et al., 2003; Brickley et al., 2005; Gilbert et al., 2006). Therefore, we have suggested that milton acts as an adaptor or regulator of the mitochondrial anterograde motor.

We demonstrate a protein apparatus that recruits kinesin to mitochondria and thereby permits anterograde movement. Milton, which interacts with both KHC and the mitochondrial protein miro, is essential in this apparatus. In contrast, kinesin light chain (KLC) is dispensable for mitochondrial transport in axons.

Results

Milton alters mitochondrial distribution

Flies that are homozygous for *milton* die as second instar larvae, and *milton* transcripts are broadly expressed in these flies, suggesting a wider role for milton than its reported function in photoreceptors (Stowers et al., 2002). Therefore, we expressed GFP fused to a mitochondrial-import signal (mitoGFP; Pilling et al., 2006) in neurons of the central nervous system to examine mitochondrial distribution in first instar larvae that are homozygous for *milt*^{92}, which is a null allele. The segmental nerves that connect the central nervous system to the body wall of the larva contain motor and sensory axons, and thereby provide the clearest structures in which to image axonal mitochondria. In control larvae, numerous mitochondria were present in these axons. However, in *milt*^{92} larvae, axonal mitochondria were absent (Fig. 1, A and B). This defect is selective for mitochondria, as indicated by the continued presence of immunoreactivity for KHC, which is likely to transport many cargoes (Goldstein, 2001; Vale, 2003), and the synaptic vesicle marker synaptotagmin (Fig. 1, C–F).

We also assayed mitochondrial distribution in the ventral nerve cord, which consists of two central neuropil regions that run the length of the cord and are surrounded by a cortex of cell bodies (Fig. 1, G and H). The neuropil regions contain axons, dendrites, and pre- and postsynaptic endings. In control larvae, mitoGFP was present in the cell bodies, but was most abundant in the neuropil, reflecting the increased concentration of mitochondria at the synapses. In the *milt*^{92} mutant, the mitoGFP pattern was reversed, with little GFP remaining in the neuropil. Synaptotagmin localization was unchanged. Thus, the selective loss of mitochondria from axons and synapses is not restricted to photoreceptors. Moreover, milton probably also mediates mitochondrial transport in dendrites because at least half of the mitochondria of the neuropil are expected to derive from postsynaptic elements.

Milton recruits KHC to mitochondria

The mitochondrial transport defect in *milton* mutants, and the in vivo association between milton and KHC, suggests that milton is an adaptor that links KHC to mitochondria. To test this hypothesis, we transfected cDNAs encoding *D. melanogaster* milton (Stowers et al., 2002) and myc-tagged rat KIF5B (myc-KHC;

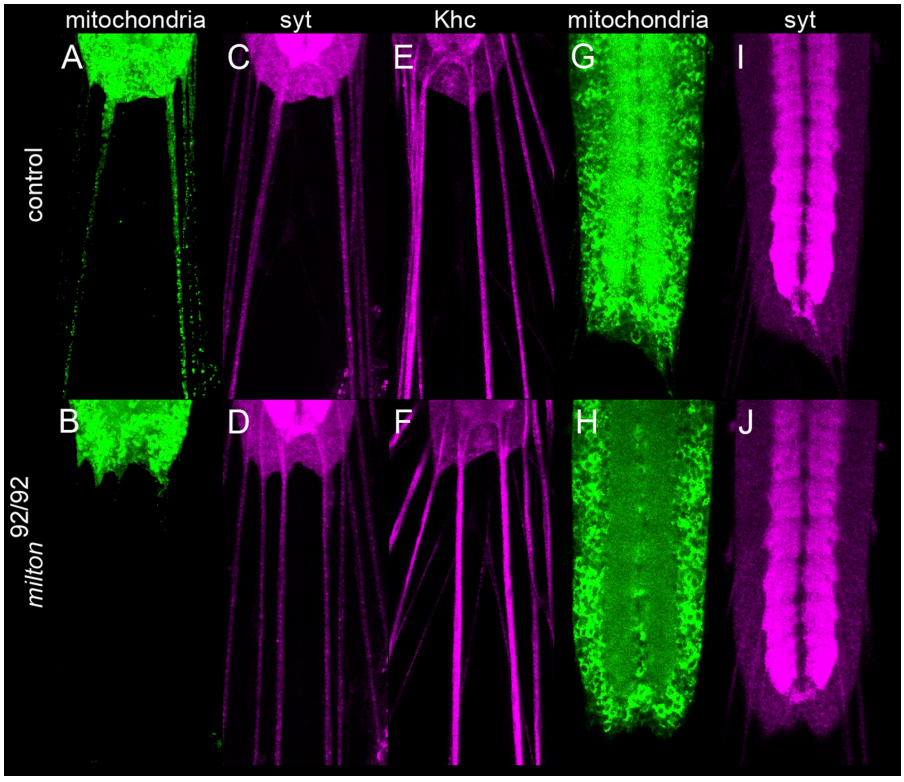

Figure 1. **Homozygous *milton* larvae lack axonal and synaptic mitochondria.** The distributions of mitochondria, synaptic vesicles, and kinesin in first instar *FRT40*, *milt*^{92}*/FRT40*, *milt*^{92} larvae (bottom row), and *FRT40/FRT40* control larvae (top row). (A–F) Examination of peripheral nerves that extend from the posterior of the nerve cord to the body-wall muscles. (A and B) GFP-labeled mitochondria are abundant in the peripheral axons in controls, but absent from *milton* axons. In contrast, anti-synaptotagmin (syt; C and D) and anti-KHC (E and F) immunolabeling of the same preparation is indistinguishable between control and mutant larvae. (G–J) Confocal images through the middle of the ventral nerve cord. (G) To either side of the midline, the synapse-rich neuropil is enriched for mitochondria (mitoGFP) in control larvae, relative to the surrounding cell-body region. (H) In *milton* nerve cords, the mitoGFP is primarily in cell bodies. (I and J) Synaptotagmin is concentrated in the neuropil of both genotypes.

Verhey et al., 1998), either alone or together, into COS7 cells. *D. melanogaster* milton and its mammalian homologues function identically in all of our assays (Fig. S2, available at http://www.jcb.org/cgi/content/full/jcb.200601067/DC1; see Mammalian milton homologues); therefore, we have used the rat kinesin in these assays. Transfected alone, milton immunoreactivity was located exclusively on mitochondria (Fig. 2 B). In untransfected cells, the endogenous KHC was typically cytoplasmic, although in some cells KHC was also observed on mitochondria. Upon transfection with milton, the KHC became highly enriched on the mitochondria, with little remaining detectable elsewhere in the cell (Fig. 3 C). The phenomenon was more dramatic when rat myc-KHC was overexpressed in these cells; myc-KHC was largely cytoplasmic, and, in some highly expressing cells, colocalized with microtubules (Fig. 2 C), as previously observed (Verhey et al., 1998). However, when cells were cotransfected with both milton and myc-KHC, KHC was overwhelmingly located on mitochondria, colocalizing precisely with both MitoTracker and milton (64 out of 66 cells; Fig. 2, D1 and D2).

In addition, mitochondrial distribution was altered by the cotransfection of milton and KHC. When milton alone was highly expressed, the mitochondria were clustered near the nucleus in 90% of the transfected cells (Fig. 2 B), which is a phenomenon encountered in only 3% of control cells. At lower expression levels, the mitochondria remained distributed as in untransfected cells (not depicted). Overall, milton expression caused less clustering of mitochondria in COS7 cells than had previously been observed in human embryonic kidney 293T (HEK293T) cells, in which all of the mitochondria become localized in an aggregate near the microtubule-organizing center (Stowers et al., 2002). In contrast, coexpression of KHC and milton caused many, though not all, mitochondria to reside at the cell margin and to form clumps at the tips of cell processes. This redistribution was not caused by a general change in the cytoskeleton. Neither KHC nor milton, transfected singly or in combination, altered the arrangement of microtubules in these cells (Fig. S1, available at http://www.jcb.org/cgi/content/full/jcb.200601067/DC1). The microtubules are chiefly oriented with plus ends toward the periphery of the cell; thus, the

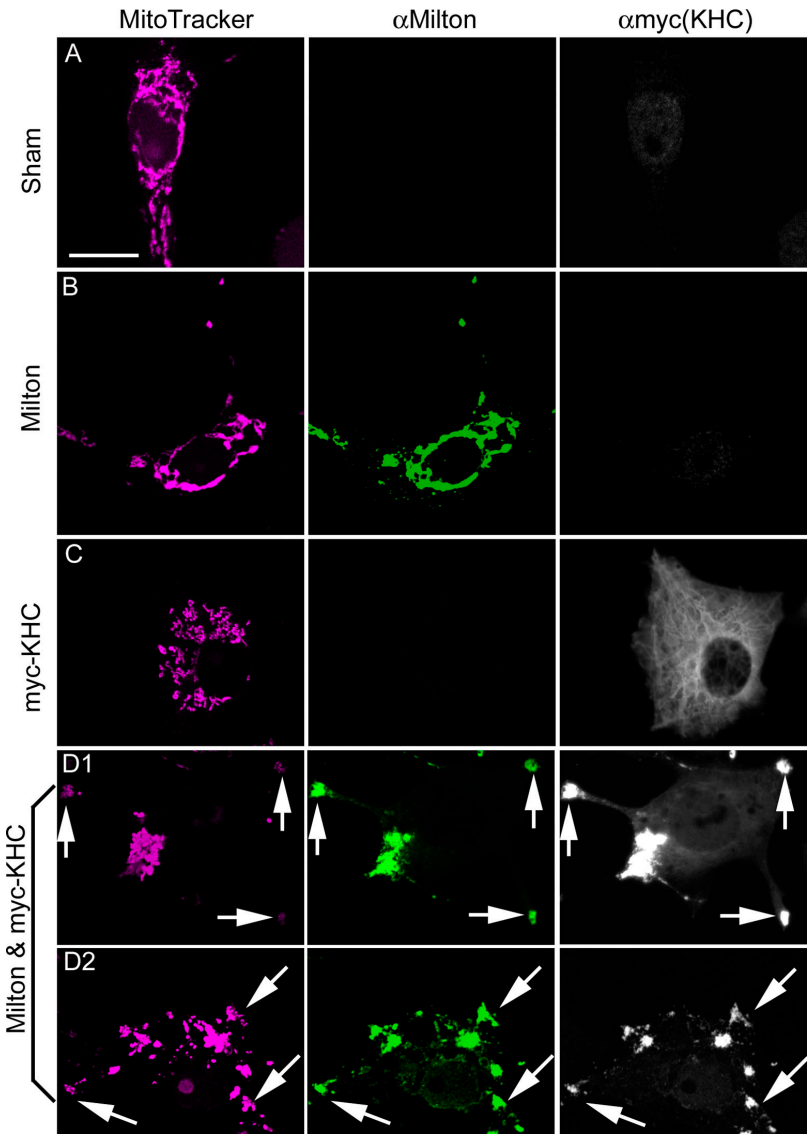

Figure 2. **Milton recruits KHC to mitochondria.** Transfected COS7 cells were immunostained with anti-milton mAb 5A124 (green) and anti-myc to detect myc-KHC (white). Mitochondria were labeled with MitoTracker orange (pink). The localization of the proteins was compared between sham-transfected cells (A) and those transfected with milton (B), myc-KHC (C), and milton and myc-KHC (D1 and D2). KHC is present in the cytosol and on microtubules in the absence of milton (B), but is recruited to mitochondria by the presence of milton (D1 and D2). Coexpression of these proteins caused mitochondria to form aggregates (arrows) that were frequently, though not always, at the periphery of the cell. Bar, 20 μm.

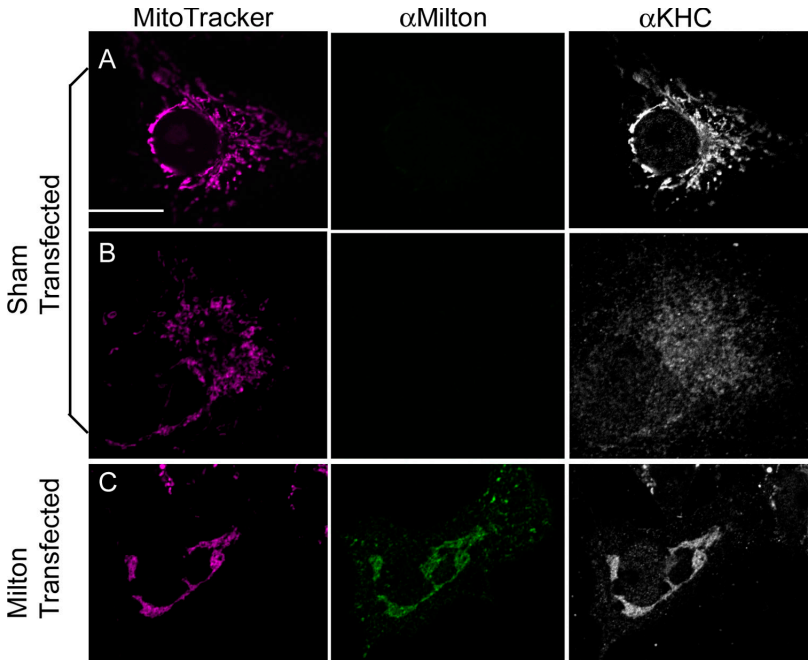

Figure 3. **Milton recruits endogenous KHC to mitochondria.** COS7 cells were immunostained with anti-KHC (white) and anti-milton (green), and mitochondria were labeled with MitoTracker orange (pink). (A and B) Control cells differed in the distribution of endogenous KHC. It was enriched on mitochondria in some (A), and had a more cytoplasmic distribution in others (B). (C) In contrast, in cells transfected with milton, endogenous KHC always colocalized with mitochondria, and little or no KHC could be detected elsewhere. Bar, 20 μm.

redistribution of mitochondria suggests that milton has recruited and activated coexpressed KHC and thereby caused a plus end–directed shift of many of the mitochondria. Together with the biochemical association of milton and KHC in *D. melanogaster* and the mitochondrial localization of milton (Stowers et al., 2002), the ability of milton to recruit KHC to mitochondria offers direct support for the hypothesis that milton is a mitochondria-specific adaptor protein for the kinesin-1 family.

Mapping the requirements for milton–KHC interactions

To further characterize the interaction between milton and myc-KHC, we mapped the region of milton that is required for their association by cotransfecting HEK293T cells and assaying the ability of portions of milton to coprecipitate with full-length myc-KHC. Milton comprises 1,116 amino acids with no recognizable structural motifs, except for a long, predicted coiled coil domain (residues 140–380) that contains a high degree of amino acid identity with the equivalent regions in mammalian milton homologues (Stowers et al., 2002). Milton 1–450 was sufficient to associate with myc-KHC. Milton 1–750 also coimmunoprecipitated with KHC, but the COOH-terminal domain of milton (Flag-tagged milton 750–1,116 and 847–1,116) did not (Fig. 4 A). We also mapped the interaction by looking for colocalization in transfected COS7 cells, whose larger cytoplasmic volume made colocalization easier to score than in HEK293T cells. Milton 1–450 colocalized with myc-KHC in aggregates, but these were not on mitochondria. In contrast, Flag-milton 750–1,116 did localize to mitochondria, but in its presence myc-KHC remained cytoplasmic (Fig. 4 C). Thus, the associations of milton with KHC and mitochondria are separable, and the 1–450 region of milton is sufficient for the interaction with KHC.

We determined the region of KHC necessary for its association with milton by cotransfecting milton with each of three truncated myc-KHC constructs and then immunoprecipitating with anti-milton mAb 5A124. Milton associated with both full-length KHC and KHC lacking the last 64 amino acids of the tail domain (myc-KHC 1–891), but not with KHC lacking the entire tail domain (myc-KHC 1–810) or a larger deletion (myc-KHC 1–682; Fig. 4 B). Therefore, the KHC tail region 810–891, but not 892–955, was necessary for associating with milton. Consistent with this finding, we observed that myc-KHC 1–891, but not 1–682, could be recruited to mitochondria by milton overexpression (Fig. 4 D).

Milton–KHC interaction is KLC independent

The kinesin-1 family, including *D. melanogaster* KHC and mammalian KIF5s, are generally considered to be tetramers composed of two KHCs and two KLCs. The deletion of amino acids 810–891 of KHC diminishes KLC binding (Verhey et al., 1998), and because endogenous KLC was present in the aforementioned experiments, milton might interact either directly with KHC or via KLC. Therefore, rat HA-tagged KLC1 (isoform C; Verhey et al., 1998) was transfected into COS7 cells both alone and in combination with KHC and milton (Fig. 5). Alone, or when transfected with milton, KLC was cytoplasmic (Fig. 5 A; Verhey et al., 1998). Even when milton, myc-KHC, and HA-KLC were coexpressed, KLC was invariably cytoplasmic and not located on mitochondria (Fig. 5 D). Moreover, in these cells, myc-KHC was also always cytoplasmic (Fig. 5 E). Thus, KLC expression inhibited the recruitment of KHC to the mitochondria by milton. We demonstrated by coimmunoprecipitation that KLC similarly inhibited the interaction of milton and KHC; HA-KLC expression prevented the coprecipitation of myc-KHC and milton (Fig. 5, F and G). Although not significantly homologous, the KHC-binding regions of milton and KLC are both predicted coiled coils and, therefore, may have similar and competing interactions for a binding site on KHC.

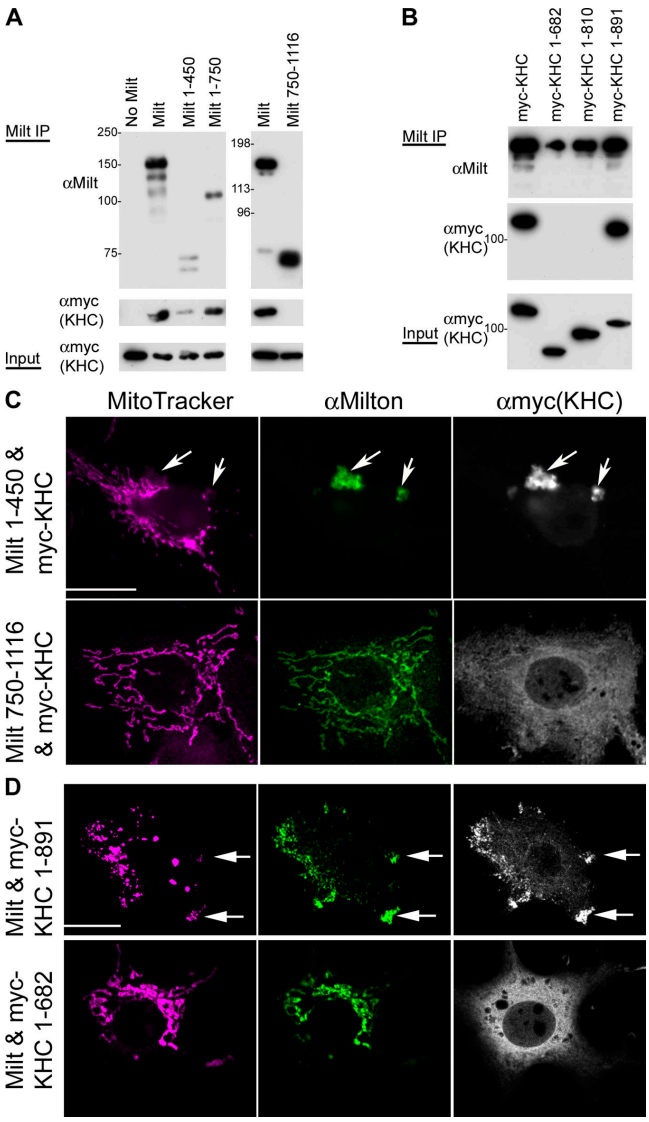

Figure 4. **The interaction of milton and KHC.** (A) Coimmunoprecipitation of truncated milton and myc-KHC from transfected HEK293T cells. (left) Cells were transfected with myc-tagged KHC and either full-length milton, milton 1–450, or milton 1–750. Total cell lysate was immunoprecipitated with anti-milton 2A108 (raised against amino acids 273–450) and probed with 2A108 and anti-myc. (right) Cotransfection with myc-KHC and either full-length milton or Flag-milton 750–1,116. Total cell lysate was immunoprecipitated with anti-milton mAb 5A124 (raised against residues 908–1,055) and then probed with 5A124 and anti-myc (KHC). (B) Coimmunoprecipitation of truncated myc-KHC and milton from lysates of HEK293T cells. Cells were transfected with milton and myc-KHC deletion constructs as indicated and immunoprecipitated with anti-milton mAb 5A124, and then the precipitate was probed with 5A124 and anti-myc. (A and B) Expression of KHC in all of the lysates was confirmed by probing the original lysate (Input) with anti-myc (KHC). In this and all subsequent figures, the autoradiograph exposures were chosen to show relative loading and protein expression levels, rather than to show the proportion of the protein in the lysate that was precipitated. (C) Milton 1–450, but not milton 750–1,116, colocalizes with KHC in COS7 cells. Anti-milton 2A108 (green) and anti-myc (KHC, white) label identical regions of cytoplasm (arrows) when KHC is expressed with milton 1–450, and these aggregates do not correspond to mitochondria labeled with MitoTracker orange (pink). Flag-tagged milton 750–1,116 (visualized with anti-milton mAb 5A124; green) and myc-KHC (white) do not colocalize, as only the former appears mitochondrial, whereas KHC remains cytoplasmic. (D) KHC 1–891, but not KHC 1–682, is recruited to mitochondria by milton. The shorter KHC remains cytoplasmic in a milton-expressing cell, whereas KHC 1–891 is associated with mitochondria, which tend to be aggregated at the margin of the cell (arrows). Bars, 20 μm.

These observations strongly suggested that KLC is not a part of the milton–KHC complex and that milton replaces KLC when associating KHC with mitochondria; therefore, we tested this hypothesis in vivo by biochemical and genetic means. As we previously observed, KHC immunoprecipitated with milton from homogenates of fly heads (Stowers et al., 2002). In these same precipitates, however, KLC was not detected. To increase the sensitivity of the assay, we immunoprecipitated milton from flies overexpressing myc-KLC (Gindhart et al., 1998). Again, KHC coimmunoprecipitated with milton, but KLC did not (Fig. 5 H). Similarly, the immunoprecipitation of myc-KLC with anti-myc brought down KHC, but milton remained in the supernatant. Immunoprecipitation with antibodies to KHC, however, brought down both myc-KLC and milton. Thus, KHC appeared to form separate complexes either with milton or with KLC; the latter are likely to be more plentiful because of the greater abundance of cargoes requiring KLC. Because the milton–KHC complex did not contain KLC, we hypothesize that milton substitutes for KHC in mitochondrial transport.

To further test the hypothesis that mitochondrial transport was KLC independent, we examined mutants lacking *klc*, which is the unique KLC gene in *D. melanogaster* (Gindhart et al., 1998). In contrast to *milton* larvae (Fig. 1), the peripheral nerves of homozygous *klc* larvae had abundant mitochondria (not depicted). Maternally contributed KLC, however, might account for the absence of a phenotype. Therefore, as a more rigorous test, we made eye clones homozygous null for *klc* (klc^{8ex94}) in a heterozygous background using the EGUF/*hid* method (Stowers and Schwarz, 1999). Loss of *klc* did not prevent the differentiation and viability of photoreceptors, although eyes were somewhat small and roughened, and their axons were frequently disordered and sometimes short and defasciculated. Nevertheless, axonal mitochondria were numerous, just as in controls, in third instar larvae (Fig. 6, A–D) and in adults (not depicted). Thus, axonal transport of mitochondria can occur in the absence of KLC. In contrast, the axons of *milton*-null photoreceptors lacked mitochondria (Fig. 6 D).

Milton splice variants are functionally distinct

Although, thus far, only a single milton cDNA; which is hereafter called milton-A, has been described (Stowers et al., 2002) and used in this paper, protein and RNA analysis suggested greater complexity. Using cDNAs and ESTs from the Berkeley *Drosophila* Genome Project, we found that milton splice variants can produce at least four distinct protein products with divergent NH_2 termini. After differing 5′ ends, the transcripts converge in exon 9, at amino acid 129 of milton-A (Fig. 7 A). Anti-milton P1–152 antibody, which was raised against amino acids 1–152 of milton-A, recognized a single band on a Western blot of *D. melanogaster* extract, but anti-milton mAb 5A124, which was raised against a domain present in all the predicted splice variants (milton-A 908–1,055), recognized multiple bands (Stowers et al., 2002). These observations are consistent with expression of splice variants in vivo.

The 129 amino acids of the NH_2 terminus of milton-A are replaced by 136 amino acids in milton-B and 269 amino acids in

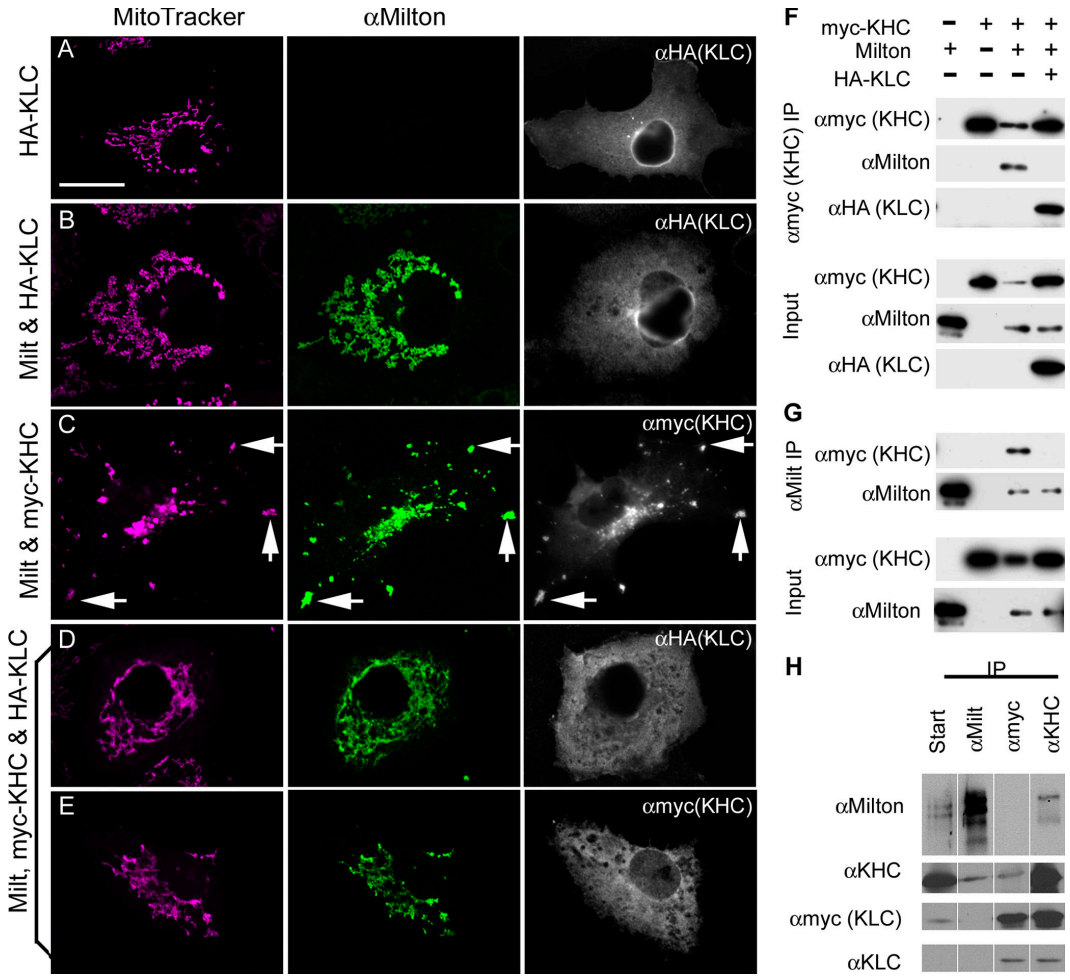

Figure 5. **Mitochondrial transport by milton and KHC is independent of KLC.** (A–E) COS7 cells, which were transfected as indicated, were immunostained with anti-milton mAb 5A124 (green) and anti-myc to detect myc-KHC (white), or with anti-HA to detect HA-KLC (white). Mitochondria were labeled with MitoTracker orange (pink). (A and B) KLC remains diffuse and cytosolic, whether or not milton is expressed. (C) In contrast, in the presence of milton, KHC was recruited to mitochondria, and, as shown in Fig. 2, mitochondria formed aggregates at the periphery of the cell (arrows). (D and E) When KLC and KHC are both expressed with milton, neither is concentrated on mitochondria, and the mitochondria remain dispersed. Bar, 20 μm. (F and G) Milton and myc-KHC do not coimmunoprecipitate in the presence of KLC. HEK293T cells were transfected with milton, myc-tagged KHC, and HA-KLC as indicated. The cell lysate was immunoprecipitated with anti-myc (KHC; F) or anti-milton mAb 5A124 (G), and immunoblots of both starting lysate (Input) and precipitates were probed with anti-myc, 5A124, and anti-HA. Milton and KHC no longer coprecipitate when KLC is coexpressed. (H) KLC is not part of the milton–KHC complex in vivo. Transgenic flies expressing myc-KLC were homogenized and immunoprecipitated with milton, anti-myc and anti-KHC. The starting homogenate and the precipitates (as labeled for each lane) were assayed as in F and G. Although milton and KHC coprecipitated with one another, KLC was associated with KHC, but not with milton. All samples were from one experiment and processed together, although they were run on more than one gel.

milton-C (Fig. 7 A). These domains have little homology to either milton-A, or to one another. In milton-D, the NH_2 terminus domain is replaced by an untranslated region, such that a translation start site corresponding to Met 138 of milton-A is predicted within exon 9. All of the predicted variants contain the predicted coiled coil domain. The National Center for Biotechnology Information databases of GenBank mRNAs and ESTs for human milton 1/OIP106 predict alternative NH_2 termini that converge at the same point as the *D. melanogaster* variants, but no alternative NH_2 termini are predicted for mammalian milton 2/GRIF-1 as yet.

Do all of the splice variants function equally in recruiting KHC to mitochondria? Each variant localized to mitochondria when transfected into COS7 cells (Fig. 7, C–E). They differed, however, in their interactions with KHC. Milton-D recruited myc-KHC to the mitochondria and coimmunoprecipitated with it (Fig. 7, B and H). Thus, milton's KHC association domain is contained within the sequences that are shared by milton-A and the shorter milton-D. Together with our earlier data (Fig. 4 A), these results indicate that the KHC association domain resides within the region corresponding to 138–450 of milton-A. Because this sequence is also present in milton-B and -C, these isoforms were likewise expected to associate with KHC and recruit it to mitochondria when equivalent amounts were expressed. Surprisingly, this was only true for milton-B (Fig. 7, B and F); milton-C neither recruited cotransfected myc-KHC to mitochondria nor coimmunoprecipitated with myc-KHC (Fig. 7, B and G).

Mammalian milton homologues

Milton's mammalian homologues function similarly to *D. melanogaster* milton, localizing to mitochondria, coprecipitating with KHC, and recruiting KHC to mitochondria (Fig. S2; Brickley et al., 2005).

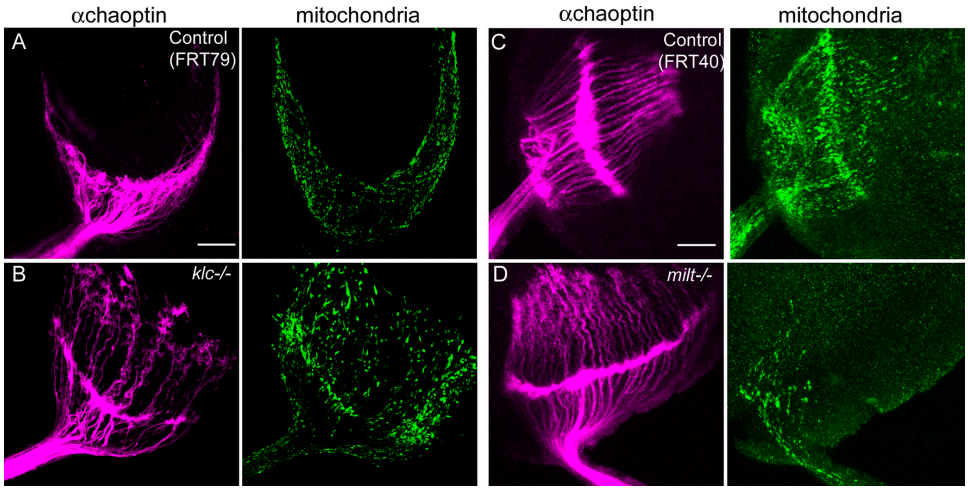

Figure 6. **Mitochondria are present in axons of *klc* null, but not in *milton* null, photoreceptors.** Eyes were engineered to derive solely from clones homozygous for either klc^{8ex94} or $milt^{92}$. Third instar larvae were dissected and photoreceptor axons were labeled with anti-chaoptin (pink) and mitoGFP expressed selectively in the photoreceptors by *ey*-GAL4. The bundled photoreceptor axons defasciculated upon innervation of the optic lobe in both controls (A and C) and mutants (B and D). (B) Although *klc* axons appear disordered, they still contain numerous mitochondria. (D) In contrast, *milt* axons project into the optic lobe more normally, but almost all of the axons lack mitochondria. A few axons do contain mitochondria, but they are likely to be heterozygous axons that persist at this developmental stage. Bars, 20 μm.

Therefore, we examined the distribution of endogenous miltons in mammalian cells by means of the P1–152 antiserum, which could recognize milton 1 and 2 because of the high conservation of the epitope (milton-A 1–152). In rat cerebellar granule neurons, endogenous milton colocalized with the mitochondrial marker cytochrome *c* oxidase (Fig. S2 E). In COS7 cells, endogenous milton was also observed on mitochondria (Fig. S2 F). Thus, *D. melanogaster* milton and its mammalian homologues are likely to play equivalent roles in mitochondrial transport.

Miro binds to milton and can affect its association with mitochondria

Despite its mitochondrial localization, milton has neither a mitochondrial import sequence nor a transmembrane domain. To examine how milton associates with mitochondria, we expressed partially deleted forms of milton. Milton's COOH terminus (expressed as either amino acids 847–1,116 or 750–1,116) had a mitochondrial distribution in COS7 cells (Fig. 8, A and B), although some remained cytoplasmic in highly expressing cells. In contrast, milton 1–450 was primarily nuclear at low expression levels (Fig. 8 C) or filled the cytoplasm in higher expressing cells (not depicted). Milton 1–750 was also cytoplasmic, although it was occasionally enriched near the nucleus (Fig. 8 D and Fig. 9 H). Thus, the COOH terminus of milton must contain a domain that is sufficient to be targeted to mitochondria.

A mitochondrial protein that might interact with milton was identified in a catalog of yeast two-hybrid interactions of *D. melanogaster* proteins (Giot et al., 2003). This protein, miro, contains two GTPase domains, a pair of EF hands, and a COOH-terminal transmembrane domain, and localizes to mitochondria (Fransson et al., 2003). When mutated, both human miro (Fransson et al., 2003) and the yeast orthologue, Gem1p (Frederick et al., 2004), alter the subcellular localization of mitochondria in a manner reminiscent of milton overexpression (Fig. 2 B). Mutations in *D. melanogaster miro* were recently isolated (Babcock et al., 2003; Guo et al., 2005) and found to lack axonal mitochondria (Guo et al., 2005). Thus, miro is likely to be another essential component of the machinery for mitochondrial transport, and, therefore, we examined its relationship with milton.

We have confirmed the interaction of miro and milton that was predicted by the two-hybrid screen by coimmunoprecipitation. HEK293T cells were transfected with milton-A or -D and either *D. melanogaster* miro that was tagged with the T7 epitope or a control T7-tagged protein. Both milton isoforms were found in anti-T7 immunoprecipitates only when T7-miro was coexpressed (Fig. 9 B). When expressed in COS7 cells, *D. melanogaster* miro invariably localized to mitochondria and induced a redistribution of mitochondria into aggregates (Fig. 9 D). This aggregation was more severe when milton was coexpressed, but was not accompanied by a change in microtubule structure (Fig. S1).

Because miro has a transmembrane domain, we hypothesized that miro might be important for the mitochondrial localization of milton and that miro lacking the transmembrane domain (miroΔTM; amino acids 1–574) might have dominant-negative effects. Unlike full-length miro, miroΔTM, when expressed in COS7 cells, was diffusely distributed throughout the cytoplasm and was also nuclear when very highly expressed. Moreover, miroΔTM did not alter mitochondrial distribution (Fig. 9 E). However, miroΔTM could still bind to milton, as indicated by their coprecipitation when cotransfected (Fig. 9 A). In contrast to the strictly mitochondrial localization of milton when expressed with full-length miro, milton was displaced from mitochondria in most cells by expression of miroΔTM (Fig. 9, F and G). Thus, miro appears to be important for the association of milton with mitochondria, perhaps by serving as a receptor for milton on the mitochondrial surface. Consistent with this hypothesis, a truncated milton (1–750), which did not associate with mitochondria when expressed alone (Fig. 9 H),

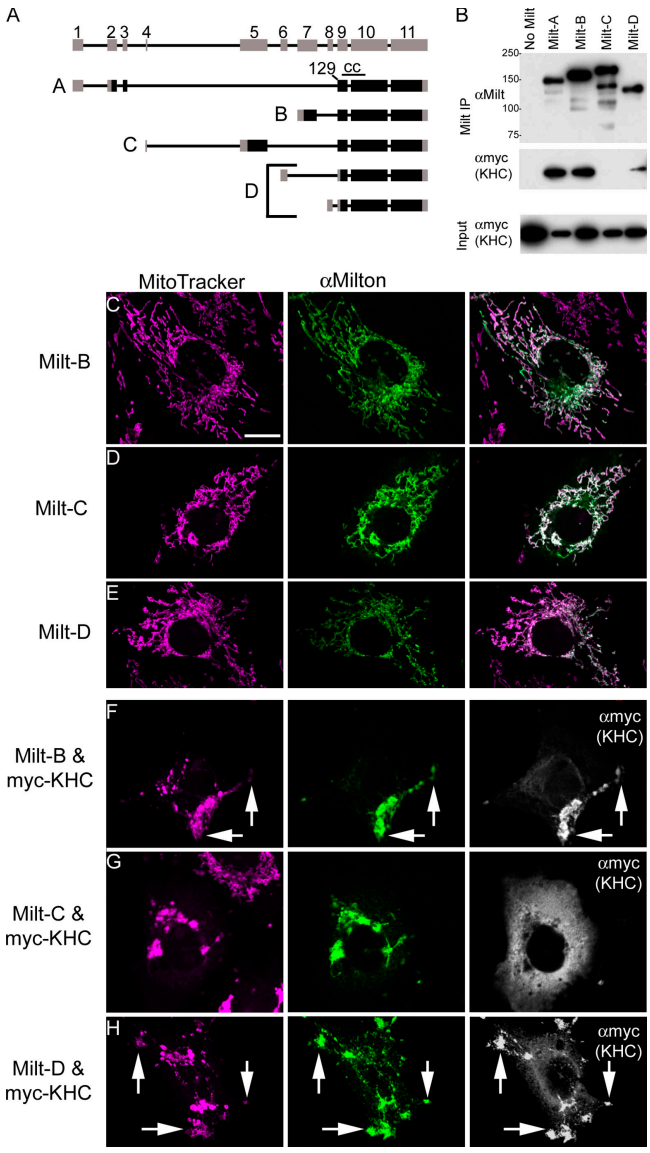

Figure 7. **Alternative splicing of milton regulates its association with KHC.** (A) Genomic structure of milton and its alternatively spliced transcripts. Milton has at least four predicted protein products (A–D) that derive from five transcripts. The transcripts share coding exons 9–11 (corresponding to amino acids 129–1,116 of the A isoform described by Stowers et al. [2002]), but differ in their 5′ ends, which are predicted to encode divergent NH_2 termini. Milton-D derives from two transcripts that differ only in their 5′ untranslated region, and its translational start site is predicted to fall within exon 9 at Met138 of milton-A. The coiled coil domain (marked CC above milton-A) is present in each variant. Translated regions are black and untranslated regions are gray. (B) Immunoprecipitates by anti-milton mAb 5A124 of HEK293T cells transfected with myc-KHC and milton-A, -B, -C, or -D as indicated. Precipitates were probed with 5A124 and anti-myc (KHC). KHC coprecipitated with milton-A, -B, and -D, but not -C. (C–E) COS7 cells were transfected with milton variants, as indicated, and anti-milton mAb 5A124 immunoreactivity (green) colocalized in each case with mitochondria labeled with MitoTracker orange (pink). Low expressing cells are shown to demonstrate milton's colocalization with mitochondria, but when milton-B, -C, and -D are highly expressed, they induce aggregation of mitochondria near the nucleus, just like milton-A. (F–H) COS7 cells were cotransfected with milton variants and myc-KHC, as indicated, and immunostained with 5A124 (green) and anti-myc (white). Milton-B and milton-D, but not milton-C, recruited KHC to the mitochondria and caused aggregation of mitochondria. (G) The aggregation of mitochondria near the nucleus reflects the high levels of milton-C expression in these cells, rather than a consistent consequence of KHC coexpression with milton-C.

was recruited to mitochondria when *D. melanogaster* miro was overexpressed in COS7 cells (Fig. 9 I). Milton 1–750 was also able to coimmunoprecipitate with miroΔTM (Fig. 9 C). Notably this milton construct does not contain the mitochondrial association domain we identified in the COOH terminus; it is therefore likely that milton associates with mitochondria through at least two regions: residues 847–1,116 bind to an unidentified protein and 1–750 bind to miro (Fig. 10).

Discussion

We have examined the involvement of milton in kinesin-mediated mitochondrial motility and, thus, in the essential process of distributing mitochondria within the cell. From these studies we have derived a model of a protein complex that includes kinesin and adaptor proteins that link kinesin to the mitochondrion (Fig. 10). These proteins are also likely to serve as a focal point for regulating mitochondrial motility.

The mechanistic basis of the *milton* phenotype

In vivo, *milton* is required for the axonal transport of mitochondria throughout the nervous system (Fig. 1; Stowers et al., 2002). Milton associates with kinesin-1 via a highly conserved domain located between residues 138 and 450. This association can recruit kinesin to mitochondria in COS7 cells and appears to activate plus end–directed transport of mitochondria, as judged by their redistribution to aggregates in the periphery of many cells transfected with both milton and KHC. These findings provide a mechanistic explanation for the absence of mitochondria from *milton* axons and terminals. Consistent with this model, the motors that endogenously associate with milton, KHC in *D. melanogaster* (Fig. 5 H; Stowers and Schwarz, 2002), and KIF5 members in mammals (Fig. 5, F and G; Brickley et al., 2005) have previously been implicated in the axonal transport of mitochondria (Hurd and Saxton, 1996; Tanaka et al., 1998).

The function of miro in mitochondrial motility

The association of milton with mitochondria appears to be mediated, in part, by its interactions with miro, and this probably accounts for the failure of mitochondrial transport in the axons of *miro* mutants (Guo et al., 2005). This proposal is supported (a) by the ability of a truncated cytosolic form of miro to act as a dominant negative and displace milton from mitochondria, and (b) by the ability of overexpressed full-length miro to recruit to mitochondria a truncated milton (residues 1–750) that could not independently localize there. However, additional interactions for tethering milton to mitochondria are likely, as a COOH-terminal portion of milton (residues 847–1,116) also localizes to the organelle. The difficulty of purifying mitochondria from limited numbers of homozygous *miro* larvae prevents a direct determination of the amount of milton on mitochondria that lack miro.

The role of *miro* in kinesin-mediated transport does not preclude additional roles for *miro*. Indeed, such functions are

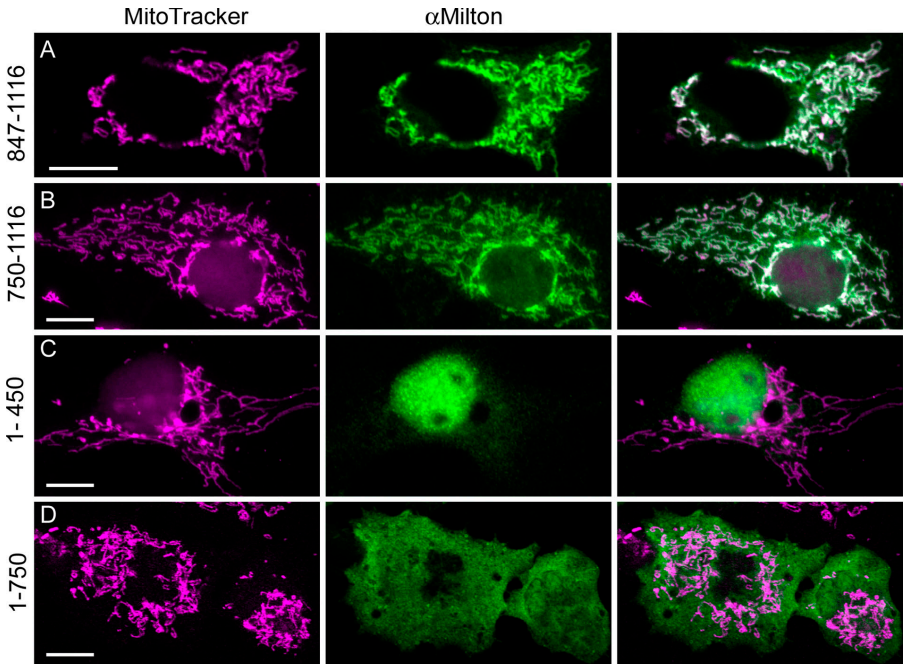

Figure 8. **Truncated milton can localize to mitochondria.** COS7 cells were transfected with either COOH-terminal regions of milton-A (amino acids 750–1,116 and 847–1,116, and also carrying a flag epitope tag) or NH_2-terminal regions (amino acids 1–450 and 1–750). Cells were labeled with MitoTracker orange and anti-milton mAb 5A124 (A and B) or 2A108 (C and D). Constructs containing the region 847–1,116 were localized to mitochondria, but those that lacked this region were not. Bar, 10 μm.

likely because a miro homologue, GEM1p, is found in yeast, where mitochondrial motility is chiefly actin-based (Yaffe, 1999; Boldogh et al., 2005), and GEM1 mutants have abnormal mitochondrial distributions (Frederick et al., 2004). In addition, it will be of interest to determine the relationship of milton and miro to syntabulin, which is another protein that has recently been proposed to link kinesin to mitochondria (Cai et al., 2005).

KLC is not needed for KHC to transport mitochondria

Unexpectedly, we found that axonal transport of mitochondria did not require the light chains of the kinesin-1 motors and that light chains were, indeed, absent from the milton–kinesin complex. When expressed in COS7 and HEK293T cells, the association between milton and KHC was inhibited by KLC. In fly homogenates, KLC was not detected in immunoprecipitates of the milton–KHC complex. Mitochondria were abundant in the axons of *klc*$^{-/-}$ photoreceptors. Thus, this mitochondrial motor provides an exception to the conventional tetrameric structure of kinesin-1. Precedent for KHC-based transport that is KLC independent has been reported in *Neurospora crassa* (Steinberg and Schliwa, 1995), sea urchins (Skoufias et al., 1994), neuronal dendrites (Setou et al., 2002), and the transport of RNA particles (Palacios and St. Johnston, 2002; Kanai et al., 2004; Ling et al., 2004).

The interaction of milton with KHC was not only KLC independent, but was inhibited by KLC overexpression in transfected COS7 and HEK293T cells. Therefore, a pool of KHC without KLC is required for milton to associate with KHC in vivo. Previous studies have found evidence for such a pool in bovine brain (Hackney et al., 1991). In light of our findings and those cited in the preceding paragraph, it may be appropriate to consider the light chains as one of several cargo adaptors for kinesin-1, of which milton is another.

The regulation of mitochondrial movement

Mitochondria are not static. In dividing cells they go through orchestrated movements to distribute themselves between the daughter cells (Yaffe, 1999). Within axons they typically alternate between stationary and moving states and can reverse their direction (Hollenbeck, 1996; Ligon and Steward, 2000a). They arrest in the presence of elevated Ca^{2+}, including Ca^{2+} that is derived from the activation of synaptic receptors (Li et al., 2004), and respond to the activation of neurotrophin receptors and various intracellular signals (Rintoul et al., 2003; Chada and Hollenbeck, 2004; Miller and Sheetz, 2004; Malaiyandi et al., 2005). It is noteworthy that, in addition to linking kinesin to the mitochondria, the milton–miro complex provides several possible mechanisms for the regulation of transport. These include the alternative splicing of milton, the posttranslational modification of milton, and the modulation of the state of miro.

We have shown that the choice of NH_2 terminus splicing variant can influence KHC's association with the adjacent region of milton. In particular, KHC did not associate with milton-C, although it contains the KHC-association domain that is common to all the isoforms. The NH_2 terminus of milton-C presumably inhibits the interaction with KHC and might, thereby, reserve a pool of mitochondria for retention in the cell body. Alternatively, the inhibition may not be constitutive in vivo, but, instead, might undergo regulation by additional factors and thereby control the recruitment of kinesin. In this context, it may be noteworthy that multiple bands of milton are detected on immunoblots from fly heads. Most of the milton isoforms in these homogenates are in an association with KHC, as determined by immunodepletion with anti-KHC. However, there is one major band, representing nearly half of the endogenous milton, which does not appear to be associated with KHC (Stowers et al., 2002). Thus, additional motors may associate with milton, and particularly with milton-C. Milton may also be

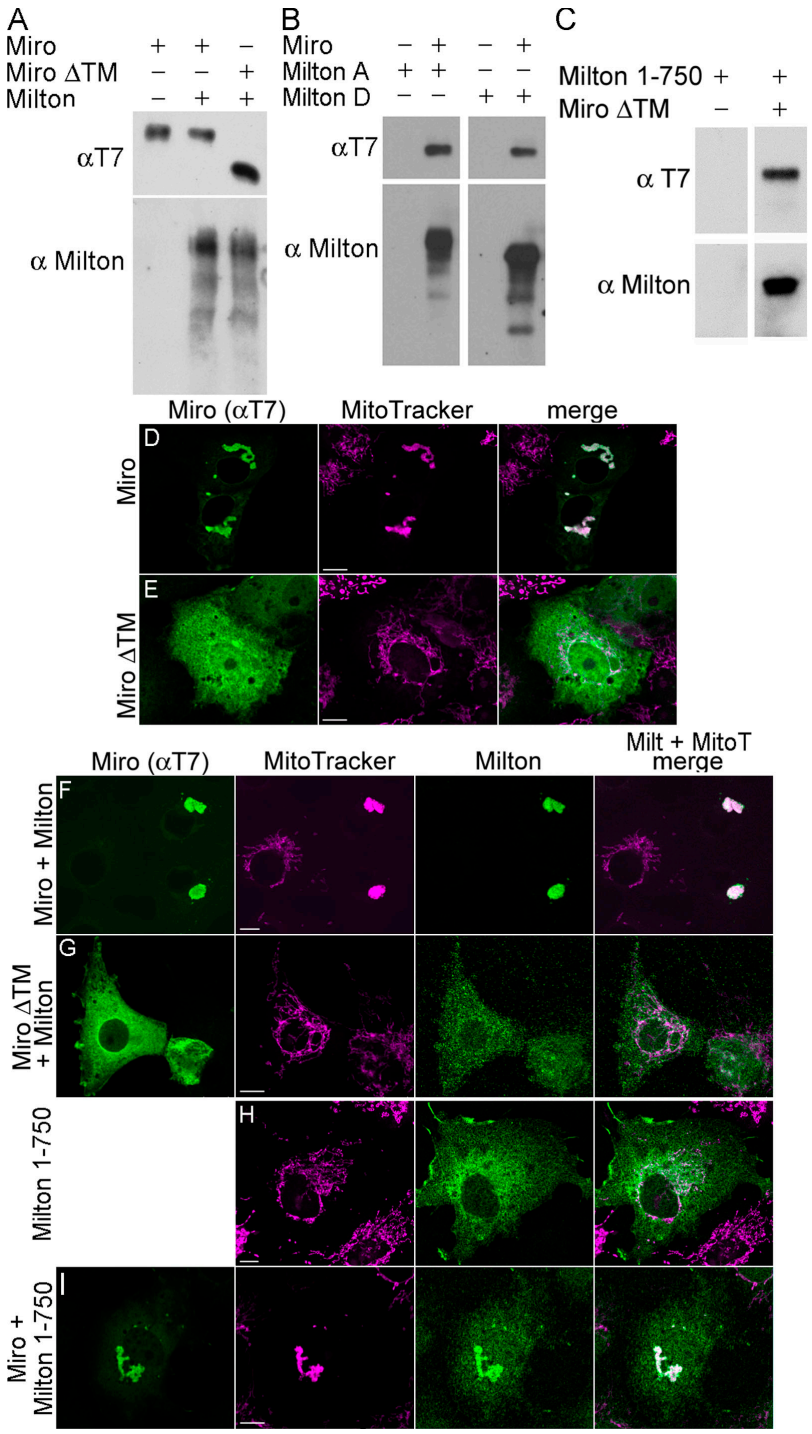

Figure 9. **Milton associates with miro, and a dominant-negative miro can displace milton from mitochondria.** (A–C) Coprecipitation of milton and T7-tagged miro constructs from transfected HEK293T cells with antibodies to T7. (A) Milton copurified with full-length miro, as well as miro lacking the COOH-terminal transmembrane domain (MiroΔTM). (B) Both milton-A and -D coprecipitated with miro. (C) Milton 1–750 coimmunoprecipitates with miroΔTM. (D and E) Full-length miro localizes to mitochondria when transfected into COS7 cells (D), but miroΔTM does not (E). (F–I) Cotransfection of full-length and truncated milton and miro constructs. Milton and miro colocalize with mitochondria when simultaneously transfected (F), but milton is displaced from mitochondria when cotransfected with miroΔTM (G). Milton 1–750 is not mitochondrially associated when expressed alone (H), however, coexpression with miro induces mitochondrial localization (I). Bar, 10 μm.

involved in such processes as mitochondrial fission and elongation, and such a role might explain the clustering of mitochondria when milton and miro are overexpressed.

The alternative splicing of milton may also represent an adaptation of the complex to the needs of particular cell types. Antiserum P1–152, which binds only to milton-A, labels a subset of the structures in the *D. melanogaster* brain that are recognized by antibodies to the common regions (Stowers et al., 2002). Thus, there is tissue specificity in the choice of splicing variant. To date, ESTs for milton-D have only been found in a testes library; therefore, milton-D may correspond to the male-specific *milton* transcripts on Northern blots (Stowers et al., 2002) and be necessary for the elongation of mitochondria along the axoneme of sperm (Siegenthaler et al., 2003).

Posttranslational modifications are also likely to regulate mitochondrial motility. In particular, the COOH-terminal portions of the mammalian miltons bind to, and are substrates for, the cytosolic glycosylating enzyme *O*-GlcNAc transferase (OGT; Iyer et al., 2003). We have identified *D. melanogaster* OGT by mass spectroscopy in immunoprecipitates of milton

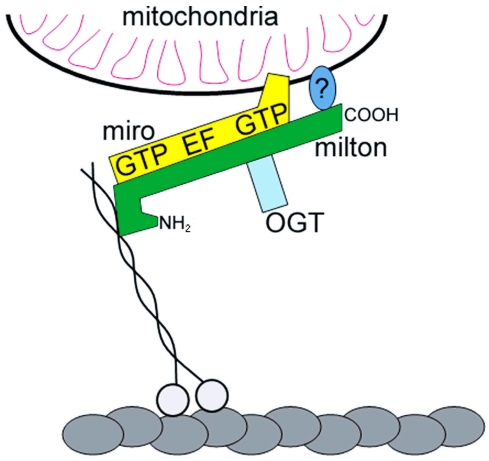

Figure 10. **Schematic representation of the protein complex that mediates anterograde mitochondrial movement.** Miro is anchored to the outer membrane by its COOH-terminal transmembrane domain. The association of milton with the mitochondrion is caused, at least in part, by the interaction of milton and miro, although an additional association via the COOH terminus of milton is also likely. Milton is associated with OGT, which is a likely regulatory enzyme, and is responsible for recruiting KHC to the mitochondrial surface. The indicated GTPase domains and EF hands of miro are also likely to regulate mitochondrial movement, as is the alternatively spliced NH_2 terminus of milton.

from fly homogenates (unpublished data). In addition, we have determined that GlcNAc-modified milton is associated with kinesin in vivo in *D. melanogaster* (unpublished data), although the physiological consequences of this conserved modification are not known.

Miro, however, may be of the greatest potential interest as a regulator of mitochondrial motility because it contains two predicted calcium-binding EF hands, which are flanked by two GTPase domains (Fransson et al., 2003; Frederick et al., 2004). Because Ca^{2+} stops mitochondrial movement, and thereby concentrates mitochondria near areas of high energy demand, such as active synapses, the EF hands of miro are likely to be particularly important.

Mitochondrial motility is a feature of most, perhaps all, eukaryotic cells. In neurons, much of this motility is microtubule based, with kinesin as the plus end–directed motor. This motility, and its regulation by a variety of signals, permits the mitochondria to be distributed in accordance with local energy use. Inadequate mitochondrial function in axons or dendrites can result in decreased synapse formation (Li et al., 2004), a failure to maintain synaptic transmission (Verstreken et al., 2005), or axonal degeneration (Ferreirinha et al., 2004). The identification of milton and miro as key components of the mechanism for mitochondrial transport by KHC should lead to a greater mechanistic understanding of the regulation of mitochondrial movement.

Materials and methods

Visualization of mitochondria

Mitochondria were visualized in *D. melanogaster* using transgenic stocks containing mitoGFP (Pilling et al., 2006) and placed under the control of a UAS promoter. Expression in selective tissues was driven by D42-Gal4, which is expressed in a subset of neurons (Fig. 1), or ey-Gal4, which is expressed in photoreceptors (Fig. 6). To visualize mitochondria in culture, cells were incubated with 100–300 nM MitoTracker orange (Invitrogen) for 15 min.

Constructs

Milton-A deletion constructs were constructed as follows: milton-A 1–450 and milton-A 1–750 were made from full-length milton-A in pCMV Tag1 (Stowers et al., 2002) that was partially digested by Sal1; milton-A 608–1,116, 750–1,116, 608–942, and 847–1,116 were made by PCR with 5′ primers containing a BamHI site and 3′ primers with HindIII sites and were cloned into pCMV Tag1 (Stratagene) with in-frame NH_2 terminus Flag tags.

Milton-B (LD33316), -C (LD28289), and -D (AT08952 and AT28977, which differ only in the 5′ untranslated region) were obtained from the Berkeley *Drosophila* Genome Project (University of California, Berkeley, CA), and their PCR-amplified NH_2 termini were substituted for that of milton-A in pCMV Tag1 milton-A. The NH_2 termini of these clones were amplified by PCR with 5′ primers containing a BamHI site and a 3′ primer with an XhoI site and cloned into BamHI–XhoI–digested pCMV Tag1 milton-A. pCMV Tag1 milton-C was made similarly, but using NotI at the 5′ instead of BamHI. Human xpress-OIP106 (milton 1) and rat xpress-GRIF-1 (milton 2) were provided by G. Hart (Johns Hopkins University, Baltimore, MD; Iyer et al., 2003). Rat myc-KHC, myc-KHC1-682, myc-KHC1-810, myc-KHC1-891, and HA-KLC constructs were provided by K. Verhey (University of Michigan, Ann Arbor, MI; Verhey et al., 1998). An EST, RE01164, corresponding to *D. melanogaster* miro (CG5410-PE), was obtained from the Berkeley *Drosophila* Genome Project and cloned between the BamHI and NotI sites of pA1T7 (Shamah et al., 2001), thereby placing a T7 epitope tag at the NH_2 terminus. MiroΔTM was generated by digesting the miro construct with EcoRI and NotI, and then ligating an oligo-encoding a stop codon between these sites.

Immunostaining

COS7 and HEK293T cells were cultured in DME supplemented with 10% FCS, L-glutamine, and penicillin/streptomycin. Rat cerebellar neurons were cultured as previously described (Sivasankaran et al., 2004). Cells were transfected with calcium phosphate and immunostained 24–36 h later. In all cotransfection experiments, 1:1 ratios of DNA were used, except for miroΔTM, which was transfected in a 250-fold excess. Immunocytochemistry was performed as previously described (Stowers et al., 2002) and used either anti-milton mAbs 2A108, 4A75, or 5A124, or anti-milton antiserum P1–152. Other primary antibodies used in this study include: chick anti-myc (Invitrogen), 9E10 (Santa Cruz Biotechnology, Inc.), chick anti-HA (GTS, Inc.), anti-Xpress (Invitrogen), goat anti-T7 (Bethyl Laboratories, Inc.), mouse anti-T7 (Novagen), anti-kinesin (AKIN01; Cytoskeleton, Inc.), anti-cytochrome *c* oxidase (BD Biosciences), rabbit anti-KLC (a gift from J. Gindhart, University of Richmond, Richmond, VA; Gindhart et al., 1998), mouse anti-HSP60 (Stressgen Bioreagents), and rabbit anti-HA (Novus Biologicals, Inc.). The following fluorescently tagged reagents were used: goat anti–mouse Alexa Fluor 488, goat anti–chick Alexa Fluor 647, donkey anti–mouse Alexa Fluor 647, donkey anti–goat Alexa Fluor 633, and donkey anti–mouse Alexa Fluor 647 (all from Invitrogen), and goat anti–mouse Cy3, horseradish peroxidase Cy5, and donkey anti–rabbit FITC (Jackson ImmunoResearch Laboratories).

Cells were imaged at room temperature (25°C) with a 63×, NA 1.4, oil Plan-Apochromat objective lens on a laser scanning confocal microscope (LSM 510 META/NLO; Carl Zeiss MicroImaging, Inc.) with LSM software 3.2 (Carl Zeiss MicroImaging, Inc.). Images were assembled into figures with Photoshop 8.0 (Adobe) using only linear adjustments of contrast and color.

First or third instar larvae were dissected in PBS, fixed in 4% formaldehyde for 20–30 min in PBS, washed three times in PBT (PBS, 0.3% Triton X-100, and 0.5% bovine albumin serum), incubated in PBTS (PBT with 5% normal donkey serum) for 30–60 min, and then incubated with 24B10 anti-chaoptin (Developmental Studies Hybridoma Bank) at 1:200 overnight in PBTS at 4°C. The preparations were washed three times in PBT, then incubated in goat anti–mouse Cy3 (Jackson ImmunoResearch Laboratories, Inc.) 1:400 in PBTS, washed three times in PBT and two times in PBS with 0.3% Triton X-100 and mounted in Vectashield (Invitrogen). Confocal images of photoreceptor axons were taken with a 40×, NA 1.3, objective (Carl Zeiss MicroImaging, Inc.).

Coimmunoprecipitation

Cells were lysed in 5 mM EDTA, 300 mM NaCl, and 50 mM Tris-HCl, pH 7.5, and a protease inhibitor cocktail set III (Calbiochem) was used at 1:1,000, 0.1 mg/ml PMSF (Sigma-Aldrich), and 1% Triton X-100 when

precipitating milton with KHC, KLC, or 0.5% Triton X-100 for miro and milton experiments. Lysates were precleared with irrelevant antibodies and protein A, incubated with anti-milton antibodies mAb 9E10 or anti-T7, and protein A–Sepharose beads (GE Healthcare) for 2–3 h at 4°C. Immunoprecipitates were separated by SDS-PAGE and transferred to nitrocellulose membranes. For immunodetection, anti-milton mAb 5A124 and anti-milton mAb 2A108 were used at 1:40; rabbit anti-KLC was used at 1:100; mAb 9E10, rabbit anti-HA, and rabbit anti-KHC were used at 1:1,000; and donkey anti–rabbit HRP and goat anti–mouse HRP were used at 1:10,000 (Jackson ImmunoResearch Laboratories, Inc.)

D. melanogaster stocks

The stocks used for these experiments were:

y,w; FRT40A, milt^{92}/CyO, y$^+$ and *yw; FRT40A* and *yw; FRT40A, GMR-hid, CL/CyO, y$^+$;;Ey-Gal4, UAS FLP/TM6, y$^+$* (Stowers et al., 2002).

y,w;; MYC-KLC Df (3L) 8ex94/TM3, Sb and *Df (3L) 8ex94/TM3, Sb* (*klc* null; provided by L. Goldstein, University of California, San Diego, CA; Gindhart et al., 1998).

y,w;; D42-Gal4UAS-MitoGFP/TM6, y$^+$ and *y,w; P(w^{+mc}, UAS mitoGFP)/CyO, y$^+$* and *y,w;; P(w^{+mc}, UAS mitoGFP)/TM6, y$^+$* (A. Pilling and W. Saxton, Indiana University, Bloomington, Indiana).

y,w;; FRT79D (III) and *y,w; Ey-Gal4, UAS Flp/CyO, y$^+$; FRT79D, GMR-hid, CL/TM6, y$^+$* (Stowers and Schwarz, 1999; Bloomington Stock Center).

The *klc*-null mutant, *Df (3L) 8ex94*, was recombined onto *FRT79D* chromosome. Recombinants were confirmed by PCR analysis and by lethality complementation analysis with *klc* alleles (*klc^{8ex25}*, *klc^{99}* and *klc^{8ex27}* were provided by J. Gindhart). The following stocks were generated for use in assaying mitochondria in *klc$^{-/-}$* photoreceptors: *w; p(UAS mitoGFP)/CyO, Actin-GFP; FRT79D;* and *w; p(UAS mitoGFP)/CyO, actin-GFP; FRT79D, Df 3L (8ex94))/TM3, Ser, actin-GFP;* and *w: Ey-Gal4, UAS Flp/CyO, actin-GFP; FRT79D, GMR-hid, CL/TM3, Ser, actin-GFP*.

Online supplemental material

Fig. S1 shows that microtubules are not disrupted in transfected cells. Fig. S2 shows that mammalian miltons colocalize with mitochondria and recruit KHC to the mitochondria. Online supplemental material is available at http://www.jcb.org/cgi/content/full/jcb.200601067/DC1.

The authors thank M. Salanga and the Developmental Disabilities Research Center Imaging Core; M. Higashi, Y. Nasrullah, and Drs. R. Teodoro, D. Allan, R. Sivasankaran, Z. He, and S. Pomeroy for their valuable assistance; Drs. J. Gindhart, L. Goldstein, D. St. Johnston, and W. Saxton for fly stocks; Drs. G. Hart and K. Verhey for constructs; and Y. Nasrullah for technical support.

This work was supported by National Institutes of Health grant RO1 GM069808. E. Glater was supported by a Predoctoral National Research Service Award fellowship.

Submitted: 13 January 2006
Accepted: 19 April 2006

References

Babcock, M.C., R.S. Stowers, J. Leither, C.S. Goodman, and L.J. Pallanck. 2003. A genetic screen for synaptic transmission mutants mapping to the right arm of chromosome 3 in *Drosophila*. *Genetics*. 165:171–183.

Beck, M., K. Brickley, H.L. Wilkinson, S. Sharma, M. Smith, P.L. Chazot, S. Pollard, and F.A. Stephenson. 2002. Identification, molecular cloning, and characterization of a novel GABAA receptor-associated protein, GRIF-1. *J. Biol. Chem.* 277:30079–30090.

Boldogh, I.R., K.L. Fehrenbacher, H.C. Yang, and L.A. Pon. 2005. Mitochondrial movement and inheritance in budding yeast. *Gene*. 354:28–36.

Brickley, K., M.J. Smith, M. Beck, and F.A. Stephenson. 2005. GRIF-1 and OIP106, members of a novel gene family of coiled-coil domain proteins: association in vivo and in vitro with kinesin. *J. Biol. Chem.* 280:14723–14732.

Cai, Q., C. Gerwin, and Z.H. Sheng. 2005. Syntabulin-mediated anterograde transport of mitochondria along neuronal processes. *J. Cell Biol.* 170:959–969.

Chada, S.R., and P.J. Hollenbeck. 2004. Nerve growth factor signaling regulates motility and docking of axonal mitochondria. *Curr. Biol.* 14:1272–1276.

Ferreirinha, F., A. Quattrini, M. Pirozzi, V. Valsecchi, G. Dina, V. Broccoli, A. Auricchio, F. Piemonte, G. Tozzi, L. Gaeta, et al. 2004. Axonal degeneration in paraplegin-deficient mice is associated with abnormal mitochondria and impairment of axonal transport. *J. Clin. Invest.* 113:231–242.

Fransson, A., A. Ruusala, and P. Aspenstrom. 2003. Atypical Rho GTPases have roles in mitochondrial homeostasis and apoptosis. *J. Biol. Chem.* 278:6495–6502.

Frederick, R.L., J.M. McCaffery, K.W. Cunningham, K. Okamoto, and J.M. Shaw. 2004. Yeast Miro GTPase, Gem1p, regulates mitochondrial morphology via a novel pathway. *J. Cell Biol.* 167:87–98.

Gilbert, S.L., L. Zhang, M.L. Forster, J.R. Anderson, T. Iwase, B. Soliven, L.R. Donahue, H.O. Sweet, R.T. Bronson, M.T. Davisson, et al. 2006. Trak1 mutation disrupts GABA(A) receptor homeostasis in hypertonic mice. *Nat. Genet.* 38:245–250.

Gindhart, J.G., Jr., C.J. Desai, S. Beushausen, K. Zinn, and L.S. Goldstein. 1998. Kinesin light chains are essential for axonal transport in *Drosophila*. *J. Cell Biol.* 141:443–454.

Giot, L., J.S. Bader, C. Brouwer, A. Chaudhuri, B. Kuang, Y. Li, Y.L. Hao, C.E. Ooi, B. Godwin, E. Vitols, et al. 2003. A protein interaction map of *Drosophila melanogaster*. *Science*. 302:1727–1736.

Goldstein, L.S. 2001. Molecular motors: from one motor many tails to one motor many tales. *Trends Cell Biol.* 11:477–482.

Gorska-Andrzejak, J., R.S. Stowers, J. Borycz, R. Kostyleva, T.L. Schwarz, and I.A. Meinertzhagen. 2003. Mitochondria are redistributed in *Drosophila* photoreceptors lacking milton, a kinesin-associated protein. *J. Comp. Neurol.* 463:372–388.

Guo, X., G.T. Macleod, A. Wellington, F. Hu, S. Panchumarthi, M. Schoenfield, L. Marin, M.P. Charlton, H.L. Atwood, and K.E. Zinsmaier. 2005. The GTPase dMiro is required for axonal transport of mitochondria to *Drosophila* synapses. *Neuron*. 47:379–393.

Hackney, D.D., J.D. Levitt, and D.D. Wagner. 1991. Characterization of alpha 2 beta 2 and alpha 2 forms of kinesin. *Biochem. Biophys. Res. Commun.* 174:810–815.

Hollenbeck, P.J. 1996. The pattern and mechanism of mitochondrial transport in axons. *Front. Biosci.* 1:d91–102.

Hollenbeck, P.J., and W.M. Saxton. 2005. The axonal transport of mitochondria. *J. Cell Sci.* 118:5411–5419.

Hurd, D.D., and W.M. Saxton. 1996. Kinesin mutations cause motor neuron disease phenotypes by disrupting fast axonal transport in *Drosophila*. *Genetics*. 144:1075–1085.

Iyer, S.P., Y. Akimoto, and G.W. Hart. 2003. Identification and cloning of a novel family of coiled-coil domain proteins that interact with O-GlcNAc transferase. *J. Biol. Chem.* 278:5399–5409.

Kanai, Y., N. Dohmae, and N. Hirokawa. 2004. Kinesin transports RNA: isolation and characterization of an RNA-transporting granule. *Neuron*. 43:513–525.

Li, Z., K. Okamoto, Y. Hayashi, and M. Sheng. 2004. The importance of dendritic mitochondria in the morphogenesis and plasticity of spines and synapses. *Cell*. 119:873–887.

Ligon, L.A., and O. Steward. 2000a. Movement of mitochondria in the axons and dendrites of cultured hippocampal neurons. *J. Comp. Neurol.* 427:340–350.

Ligon, L.A., and O. Steward. 2000b. Role of microtubules and actin filaments in the movement of mitochondria in the axons and dendrites of cultured hippocampal neurons. *J. Comp. Neurol.* 427:351–361.

Ling, S.C., P.S. Fahrner, W.T. Greenough, and V.I. Gelfand. 2004. Transport of *Drosophila* fragile X mental retardation protein-containing ribonucleoprotein granules by kinesin-1 and cytoplasmic dynein. *Proc. Natl. Acad. Sci. USA*. 101:17428–17433.

Malaiyandi, L.M., O. Vergun, K.E. Dineley, and I.J. Reynolds. 2005. Direct visualization of mitochondrial zinc accumulation reveals uniporter-dependent and -independent transport mechanisms. *J. Neurochem.* 93:1242–1250.

Miller, K.E., and M.P. Sheetz. 2004. Axonal mitochondrial transport and potential are correlated. *J. Cell Sci.* 117:2791–2804.

Minin, A.A., A.V. Kulik, F.K. Gyoeva, Y. Li, G. Goshima, and V.I. Gelfand. 2006. Regulation of mitochondria distribution by RhoA and formins. *J. Cell Sci.* 119:659–670.

Morris, R.L., and P.J. Hollenbeck. 1993. The regulation of bidirectional mitochondrial transport is coordinated with axonal outgrowth. *J. Cell Sci.* 104:917–927.

Morris, R.L., and P.J. Hollenbeck. 1995. Axonal transport of mitochondria along microtubules and F-actin in living vertebrate neurons. *J. Cell Biol.* 131:1315–1326.

Nangaku, M., R. Sato-Yoshitake, Y. Okada, Y. Noda, R. Takemura, H. Yamazaki, and N. Hirokawa. 1994. KIF1B, a novel microtubule plus end-directed monomeric motor protein for transport of mitochondria. *Cell*. 79:1209–1220.

Palacios, I.M., and D. St Johnston. 2002. Kinesin light chain-independent function of the Kinesin heavy chain in cytoplasmic streaming and posterior localisation in the *Drosophila* oocyte. *Development*. 129:5473–5485.

Pereira, A.J., B. Dalby, R.J. Stewart, S.J. Doxsey, and L.S. Goldstein. 1997. Mitochondrial association of a plus end-directed microtubule motor expressed during mitosis in *Drosophila*. *J. Cell Biol.* 136:1081–1090.

Pilling, A.D., D. Horiuchi, C.M. Lively, and W.M. Saxton. 2006. Kinesin-1 and dynein are the primary motors for fast transport of mitochondria in *Drosophila* motor axons. *Mol Biol Cell.* 17:2057–2068.

Rintoul, G.L., A.J. Filiano, J.B. Brocard, G.J. Kress, and I.J. Reynolds. 2003. Glutamate decreases mitochondrial size and movement in primary forebrain neurons. *J. Neurosci.* 23:7881–7888.

Setou, M., D.H. Seog, Y. Tanaka, Y. Kanai, Y. Takei, M. Kawagishi, and N. Hirokawa. 2002. Glutamate-receptor-interacting protein GRIP1 directly steers kinesin to dendrites. *Nature*. 417:83–87.

Shamah, S.M., M.Z. Lin, J.L. Goldberg, S. Estrach, M. Sahin, L. Hu, M. Bazalakova, R.L. Neve, G. Corfas, A. Debant, and M.E. Greenberg. 2001. EphA receptors regulate growth cone dynamics through the novel guanine nucleotide exchange factor ephexin. *Cell*. 105:233–244.

Siegenthaler, M.M., R.S. Stowers, and K.G. Hales. 2003. Role of *milton* in mitochondrial morphogenesis during *Drosophila* spermatogenesis. *In* 44th Annual *Drosophila* Research Conference. Genetics Society of America, Chicago, Illinois.

Sivasankaran, R., J. Pei, K.C. Wang, Y.P. Zhang, C.B. Shields, X.M. Xu, and Z. He. 2004. PKC mediates inhibitory effects of myelin and chondroitin sulfate proteoglycans on axonal regeneration. *Nat. Neurosci.* 7:261–268.

Skoufias, D.A., D.G. Cole, K.P. Wedaman, and J.M. Scholey. 1994. The carboxyl-terminal domain of kinesin heavy chain is important for membrane binding. *J. Biol. Chem.* 269:1477–1485.

Steinberg, G., and M. Schliwa. 1995. The Neurospora organelle motor: a distant relative of conventional kinesin with unconventional properties. *Mol. Biol. Cell*. 6:1605–1618.

Stowers, R.S., and T.L. Schwarz. 1999. A genetic method for generating *Drosophila* eyes composed exclusively of mitotic clones of a single genotype. *Genetics*. 152:1631–1639.

Stowers, R.S., L.J. Megeath, J. Gorska-Andrzejak, I.A. Meinertzhagen, and T.L. Schwarz. 2002. Axonal transport of mitochondria to synapses depends on milton, a novel *Drosophila* protein. *Neuron*. 36:1063–1077.

Tanaka, Y., Y. Kanai, Y. Okada, S. Nonaka, S. Takeda, A. Harada, and N. Hirokawa. 1998. Targeted disruption of mouse conventional kinesin heavy chain, kif5B, results in abnormal perinuclear clustering of mitochondria. *Cell*. 93:1147–1158.

Vale, R.D. 2003. The molecular motor toolbox for intracellular transport. *Cell*. 112:467–480.

Verhey, K.J., D.L. Lizotte, T. Abramson, L. Barenboim, B.J. Schnapp, and T.A. Rapoport. 1998. Light chain-dependent regulation of kinesin's interaction with microtubules. *J. Cell Biol.* 143:1053–1066.

Verstreken, P., C.V. Ly, K.J. Venken, T.W. Koh, Y. Zhou, and H.J. Bellen. 2005. Synaptic mitochondria are critical for mobilization of reserve pool vesicles at *Drosophila* neuromuscular junctions. *Neuron*. 47:365–378.

Werth, J.L., and S.A. Thayer. 1994. Mitochondria buffer physiological calcium loads in cultured rat dorsal root ganglion neurons. *J. Neurosci.* 14:348–356.

Wong-Riley, M.T., and C. Welt. 1980. Histochemical changes in cytochrome oxidase of cortical barrels after vibrissal removal in neonatal and adult mice. *Proc. Natl. Acad. Sci. USA*. 77:2333–2337.

Wozniak, M.J., M. Melzer, C. Dorner, H.U. Haring, and R. Lammers. 2005. The novel protein KBP regulates mitochondria localization by interaction with a kinesin-like protein. *BMC Cell Biol.* 6:35.

Yaffe, M.P. 1999. The machinery of mitochondrial inheritance and behavior. *Science*. 283:1493–1497.

Yaffe, M.P., N. Stuurman, and R.D. Vale. 2003. Mitochondrial positioning in fission yeast is driven by association with dynamic microtubules and mitotic spindle poles. *Proc. Natl. Acad. Sci. USA*. 100:11424–11428.

Zucker, R.S. 1999. Calcium- and activity-dependent synaptic plasticity. *Curr. Opin. Neurobiol.* 9:305–313.